THE JOURNAL OF BIOLOGICAL CHEMISTRY
Vol. 278, No. 33, Issue of August 15, pp. 30881–30888, 2003
Printed in U.S.A.

RelA Control of IκBα Phosphorylation

A POSITIVE FEEDBACK LOOP FOR HIGH AFFINITY NF-κB COMPLEXES*

Received for publication, December 2, 2002, and in revised form, March 7, 2003
Published, JBC Papers in Press, March 27, 2003, DOI 10.1074/jbc.M212216200

Lin Yang‡§, Kehinde Ross‡, and Eva E. Qwarnstrom‡¶‖

From the ‡Cell Biology Unit, Functional Genomics, Division of Genomic Medicine, The Medical School, University of Sheffield, Sheffield S10 2JF, United Kingdom and the ¶Department of Pathology, School of Medicine, University of Washington, Seattle, Washington 98195

NF-κB-IκB complex formation regulates the level and specificity of NF-κB activity. Quantitative analyses showed that RelA-NF-κB-induced IκBα binding is regulated through inhibitor retention and phosphorylation. RelA caused an increase in IκBα phosphorylation and in degradation, which was enhanced monotonically with inhibitor concentration. *In vivo* analysis demonstrated the RelA-induced IκBα/RelA interactions to be specific, saturable, and phosphorylation-dependent. In addition, it showed that phosphorylation regulates both the level and affinity of the complexes and demonstrated an increased average affinity to coincide with reduction in the level of complexes during cytokine-induced pathway activation. The data show that RelA regulation of NF-κB-IκBα complex formation is IκBα phosphorylation-dependent and that IκBα/NF-κB binding is dynamic and determined by concentration of the subunits. In addition, they suggest that regulation of both complex levels and affinities through phosphorylation, with effects on the system steady state, participate in selective activation of the NF-κB pathway.

NF-κB transcription factors are central to inflammatory and immune responses (1–3). They are composed of homo- and heterodimers of a family of at least five related subunits, characterized by a ~300-amino acid Rel homology domain (4). Activation is controlled by IκB (inhibitor of NF-κB) proteins, the degradation of which is a critical step in activation of NF-κB (5). The IκB family includes seven proteins containing multiple ankyrin-like repeats, which mediate interaction with the Rel homology regions of NF-κB dimers. IκBα, the most extensively studied protein in this family, interacts primarily with p50/RelA and p50/c-Rel heterodimers but also with c-Rel and RelA homodimers (4, 6). IκBα inhibits NF-κB activation by masking its nuclear localization signals and thereby sequestering the two proteins in the form of complexes in the cytoplasm (7).

Induction of the pathway is mediated by a significant number of stimuli, including cytokines, lipopolysaccharides, cellular stress, and cell adhesion (4, 8, 9). During activation, NF-κB is transported into the nucleus and activates transcription of genes bearing cognate binding motifs (4). Transport is made possible by dissociation of complexes following phosphorylation of IκB on serines 32 and 36 by IκB kinases, ubiquitination, and proteosome degradation (10–13). The significance of IκB/NF-κB interactions as a regulatory step in pathway activation has been extensively documented (6, 14–16).

Here we report the use of the fusion protein IκBαEGFP[1] to examine regulation of the function of IκBα by NF-κB. RelA regulation of IκBα and of IκBα/NF-κB interactions were analyzed in single living cells, using confocal microscopy, showing that all aspects of IκBα function are critically dependent on that of NF-κB and that phosphorylation of the inhibitor constitutes the basis for interaction and selection during pathway activation.

EXPERIMENTAL PROCEDURES

Plasmids—The plasmid *pIκBαEGFP* encodes a red-shifted variant of green fluorescent protein fused to the carboxyl terminus of IκBα, constructed by cloning the IκBα cDNA from *pIκBα* ctag (kind gift from Prof. Ronald Hay) (17) digested with *Bam*HI plus *Eco*RI into *pEGFP-N2* (Clontech) digested with *Bgl*II plus *Eco*RI and in-filling of a *Sma*I plus *Eco*RI digest for alignment of the reading frame. Plasmid *pIκBαEYFP* was constructed by subcloning the same IκBα fragment into *pEYFP-N1* (Clontech), digested with *Bgl*II plus *Eco*RI as described (18). Plasmid *pECFPrelA* was constructed by cloning the RelA cDNA from *pBluescript-relA* (19), digested with *Hin*dIII plus *Bam*HI, into similarly prepared *pECFP-C1* (Clontech). Plasmid *pECFPp50* was constructed by cloning the p50 cDNA from *pRSV-NFκB1(p50)* (19) digested with *Hin*dIII plus *Bgl*II into *pECFP-C1* (Clontech) and in-filling of the *Xho*I site. Site-directed mutagenesis of *pIκBαEGFP* (Ser → Ala at positions 32 and 36) was performed using the Muta-Gene Phagemid kit (Bio-Rad). Mutagenesis of *pECFPrelA* to obtain nonfluorescent fusion proteins was performed by deletion of residues 65–67 (Thr, Trp, and Gly) within the ECFP N terminus, critical for fluorescence, using the QuikChange™ site-directed mutagenesis kit (Stratagene). Oligonucleotides were synthesized from Life Technologies. All constructs were confirmed by sequence analysis.

Tissue Culture and Transfection—Human gingival fibroblasts (HGFQ1 and HGFQ2, transfer 10–19) and HeLa cells were maintained in Dulbecco's modified Eagle's medium (Invitrogen) containing 10% fetal calf serum (Invitrogen) and 5 mM sodium pyruvate, 100 μg/ml penicillin and streptomycin and kept at 37 °C in a 95% O_2, 5% CO_2 atmosphere. Cells were plated 24 h prior to transfection and transiently transfected using calcium phosphate co-precipitation with glycerol shock (60 s, 15% glycerol in phosphate-buffered saline) 4 h after transfection, as described previously (20, 21). Control experiments demonstrated that transfection of mediators of the NF-κB pathway, under these conditions, had no effect on endogenous cytokine production, which was significant for pathway activation (20–22). Stimulation with IL-1 (1 nM) kindly provided by Dr. Steve Poole (National Institute of

* The confocal microscopy facility in the Section of Functional Genomics, University of Sheffield, UK, was co-funded by the Wellcome Trust, the Medical Research Council, and the Arthritis Research Campaign. This work was supported by grants from The Nuffield Foundation and The British Heart Foundation (to E. E. Q.). The costs of publication of this article were defrayed in part by the payment of page charges. This article must therefore be hereby marked "*advertisement*" in accordance with 18 U.S.C. Section 1734 solely to indicate this fact.

§ Present address: Dept. of Pathology, Brigham and Women's Hospital, Harvard Medical School, 221 Longwood Ave., Boston, MA 02115.

‖ To whom correspondence should be addressed: Cell Biology Unit, Div. of Genomic Medicine, Royal Hallamshire Hospital, Glossop Road, University of Sheffield, Sheffield S10 2JF, UK.

[1] The abbreviations used are: EGFP, enhanced green fluorescent protein; IL-1, interleukin-1; FRET, fluorescence resonance energy transfer; GFP, green fluorescent protein; ECFP, enhanced cyan fluorescent protein; EYFP, enhanced yellow fluorescent protein.

Biological Standards and Control) was carried out 24 h after transfection, for various times, as indicated.

Confocal Microscopy—EGFP fusion proteins were visualized using a confocal laser-scanning microscope (Molecular Dynamics, CLSM 2010) fitted with a 37 °C stage incubator and coupled to a Nikon Diaphot 300 microscope and a Silicon Graphics work station. Laser power was set to 10 mW, band selection to 488 nm, photo multiplier tube voltage to 750, and varying laser attenuation to maintain pixel density below 200, within the linear range of the instrument. Emission scans were done with a × 60 Plan Apo oil immersion objective (numerical aperture of 1.4) and a 50-μm aperture generating an optical section of 0.54 μm and using a 530-nm band pass filter. To quantitate the cytoplasmic and the nuclear fusion protein level, transfected cells were scanned horizontally through the nucleus, and images were analyzed using NIH Image. Relative fluorescence was calculated by measuring mean intensity of representative areas of nucleus or cytoplasm and normalized by dividing by the attenuation and further by 2.41 for consistency with previous results obtained with a photo multiplier tube of 666 V (20).

Western Analysis—The relative levels of endogenous and exogenous IκBα were determined by Western analyses as described (20) using cells transfected with ctag-containing, or fluocrome-tagged (*pEGFP*, *pEYFP*, *pECFP*, *pIκBαEYFP*, or *pECFPrelA*) NF-κB signaling components to make it possible to distinguish endogenous and exogenous proteins. Cell extracts were prepared by lysis in 1× Laemmli sample buffer (23), resolved on 12.5% SDS-PAGE, and transferred to polyvinylidene difluoride membrane (Amersham Biosciences) with β-actin used as an internal control. Total and phosphorylated IκBα were detected using primary rabbit polyclonal anti-IκBα and anti-phospho-IκBα (1:5,000; BioLab), ECFPrelA using goat anti-RelA IgG (1:10,000; Santa Cruz Biotechnology, Inc., Santa Cruz, CA), EGFP and its variants using rabbit anti-GFP IgG (Santa Cruz Biotechnology), and β-actin using mouse anti-actin IgG (Sigma), followed by horseradish peroxidase-conjugated secondary antibodies (1:2000), and visualized by ECL (Amersham Biosciences) according to the manufacturer's instructions. Quantitation of exogenous and endogenous expression levels of the various IκBα and RelA proteins was done of cells transfected with constructs containing the untagged inserts and those transfected with *pIκBαEGFP* or *pEGFPrelA* for confocal microscopy and with *pIκBαEYFP* or *pECFPrelA* for fluorescence resonance energy transfer (FRET) analysis as well as with empty vectors (*pEGFP*, *pEYFP*, and *pECFP*). Band intensity was compared with a range of concentrations of purified EGFP, and data were analyzed using NIH Image. These experiments validated the comparative use of these various constructs and showed that expression levels of untagged proteins RelA and p50 following transfection, relative to levels of the corresponding fluorescence-tagged fusion protein were 80 ± 6 and 120 ± 15%, respectively. In addition, they demonstrated that the tagged and untagged NF-κB fusions had the same effects on IL-1-induced IκBα turnover.

Immunofluorescence—Immunofluorescent staining of transfected cells was carried out as described previously (20). Briefly, incubation with a rabbit polyclonal IκBα antiserum (1 μg/ml, 1 h, room temperature; Santa Cruz Biotechnology) of cells transfected with IκBαEGFP was carried out following fixation in methanol (−20 °C, 5 min) and incubation in blocking serum (5%, 1 h) and prior to incubation with biotinylated secondary antibody (2 μg/ml, overnight at 4 °C; Santa Cruz Biotechnology) and streptavidin/Texas Red (0.2 μg/ml, 15 min; Amersham Biosciences). Data (red fluorescence) were acquired using 750 V with excitation at 568 nm and emission at 590 nm. Excitation and emission of green fluorescence from the fusion protein was done at 488 and 530 nm, respectively, as above. Green and red fluorescence was plotted for individual cells over a range of transfection levels. The level of GFP fluorescence was corrected for minor reduction in intensity (15%) induced by methanol fixation.

Immunoprecipitation—Biochemical analysis of complex formation was carried out by immunoprecipitation using an anti-RelA antibody (Santa Cruz Biotechnology), followed by Western analysis, as above, of cells transfected with wild type and mutant *pIκBαEYFP*, alone or together with *pCMV:relA*, before and after IL-1 stimulation. Thus, HeLa cells seeded at 3×10^6 cells/10-cm plate were transfected with the indicated cDNAs, totaling 4.4 μg/plate, and after 24 h they were left unstimulated or treated with IL-1β for 8 and 40 min and lysed. Immunoprecipitation of cell lysates, as above, was performed by incubating with 5 μg of anti-RelA antibody and protein G conjugated to Sepharose beads (overnight, 4 °C; Sigma). Following resuspension in lysis buffer, precipitates were separated by gel electrophoresis (20% SDS, Tris-HCl) and transferred to polyvinylidene difluoride membranes for Western analysis, as above.

FRET Analysis—Images of ECFP, EYFP, and FRET were obtained through a × 60 Plan Apo oil immersion objective (numerical aperture of 1.4) using a Nikon Diaphot 300 microscope and recorded by a 12-bit Hamamatsu digital camera C4742-95 driven by OpenLab software (Improvision). Complex formation was determined through measuring close association of fluorophores ECFP and EYFP by excitation of the donor, resulting in an increase in acceptor emission fluorescence and/or a decrease in donor fluorescence due to FRET (24–26) using a series of filter sets (Omega Optical): XF114 for ECFP (440DF21 excitation, 455DRLP dichroic, 480DF30 emission), XF104 for EYFP (500DF25 excitation, 525DRLP dichroic, 545DF35 emission), and XF88 for FRET (440DF21 excitation, 455DRLP dichroic, 545DF35 emission). Relative fluorescence was calculated for the various emission settings by measuring the mean intensity of representative areas of nucleus or cytoplasm and normalized by dividing by attenuation, as above. All images were corrected for background, and FRET images were further processed by subtracting overspill of ECFP (50.7%) and EYFP (30.4%) fluorescence assessed using vectors containing ECFP or EYFP only. The accuracy of the FRET signal was further confirmed by inhibition of emission at 545 nm after photobleaching the acceptor-EYFP at 500-nm excitation. In addition, control experiments included demonstration of a correlation between the reduction in yellow fluorescence and increase in cyan intensity.

Binding Analyses—The level of IκB/RelA binding was measured by FRET following co-transfection with IκBαEYFP (yellow fluorescence) and ECFPrelA (cyan fluorescence), before and after IL-1 stimulation (30 min) in four independent experiments. The FRET signal from single transfected cells expressing a range of IκBα or S32A/S36A-phosphodeficient IκBα mutant (ligand) concentrations was quantitated, as reported for assessment of protein/protein interactions in a variety of systems in live cells (27–30). Analysis was limited to including cells expressing levels of fusion protein of up to 8–10 times that of the endogenous levels, corresponding to fluorescence of 2.5–3, to ascertain reliable cytokine responses (20, 21). Readings were ranked according to yellow fluorescence (IκBαEYFP), and to increase accuracy, they were pooled in consecutive groups of three for data analysis. The specificity of the interaction was demonstrated by competition of the IκBαEYFP/ECFPrelA binding, carried out by co-transfecting with increasing levels of *pCMV:relA* or *pCMV:p50*, or using a mutant *pECFPrelA* lacking the cyan fluorescent site. Saturated binding and apparent dissociation constants were estimated by nonlinear least squares fitting of a noncooperative one-site equilibrium-binding model of the FRET *versus* IκBα (yellow fluorescence). All data were analyzed using MLAB for the Macintosh (Civilized Software, Silver Spring, MD).

Cellular concentrations of the various fusion proteins were determined by Western analysis of transfected cells as above and were included in calculations of binding affinity (K_a) using the equation,

$$\text{Bound (molecules/cell)} = \frac{\text{Receptor} \times K_a \times [\text{Ligand}]}{1 + K_a \times [\text{Ligand}]} \qquad \text{(Eq. 1)}$$

where Bound (molecules/cell) represents the level of bound IκBα/cell determined by FRET; Receptors/cell or Binding protein is RelA concentration (molecules/cell); and [Ligand] is IκBα concentration (molecules/cell).

Controls included calculations using various size pools for data analysis (groups of 3–6), as well as using larger data sets allowing up to 12 individual cell readings for each IκBα concentration, all demonstrating the same results as regards specific binding sites and affinity values. In addition, the single cell analysis was assessed by determining the R^2 values. These were found to be of the same order as that obtained from conventional binding analysis, varying by 15 ± 5%, demonstrating a high level of accuracy, and further revealing an underlying Gaussian distribution as regards cell/cell variation.

RESULTS

Kinetic analysis of single cell data obtained by confocal microscopy demonstrated a pronounced enhancement of IκBαEGFP degradation by co-transfection with RelA alone or together with p50, increasing IL-1-induced turnover from 60 to 90–95% (Fig. 1, *A* and *B*). In contrast, levels of a serine 32/36 phosphorylation-deficient IκBα mutant (31–33) were unaffected by IL-1 stimulation, either when transfected alone or following co-transfection with NF-κB subunits. In addition, there was a positive correlation between the magnitude of the effect and the initial cytoplasmic levels of IκBα (Fig. 1*C*).

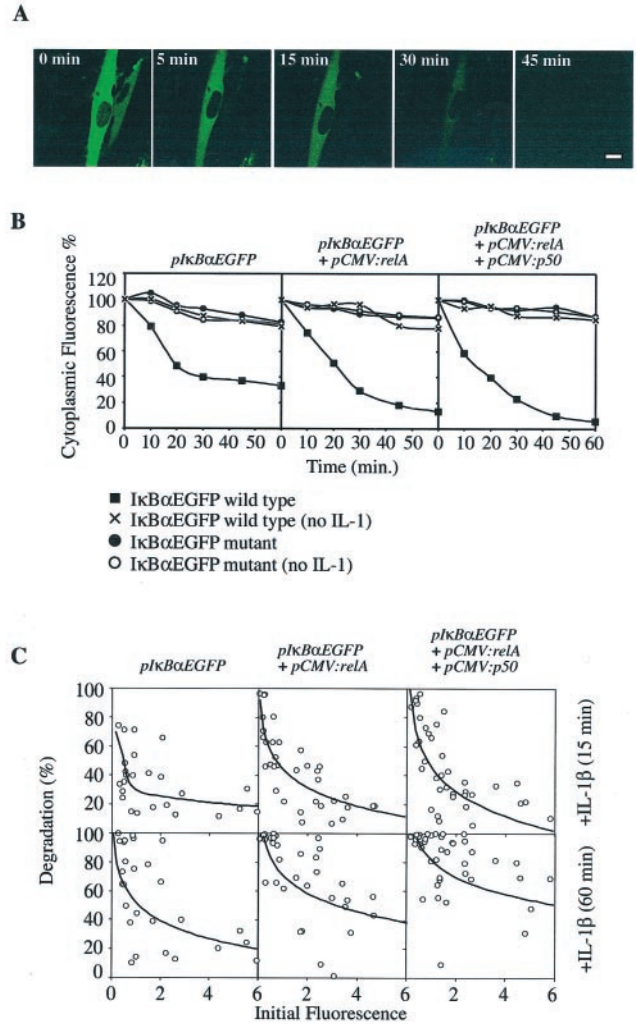

FIG. 1. **NF-κB enhances IL-1-stimulated inhibitor degradation at high levels of IκBα.** *A*, series of confocal images of fibroblasts, co-transfected with equal amounts of *pIκBαEGFP* and *pCMV:relA*, obtained at various times after the addition of IL-1β as indicated. Bar, 20 μm. *B*, average IκBαEGFP levels were determined at various times during IL-1β stimulation and transfected with *pIκBαEGFP* or a mutant *pIκBαEGFP*, lacking phosphorylation sites at serines 32 and 36, alone or co-transfected with *pCMV:relA*, or with *pCMV:relA* and *pCMV:p50*. *C*, the percentage degradation of the IκBαEGFP fusion protein following transfection with *pIκBαEGFP* alone or together with *pCMV:relA* or together with *pCMV:relA* and *pCMV:p50*, following 15- or 60-min stimulation with IL-1β, was determined for individual cells and plotted against initial fluorescence. A best fit logarithmic curve to the data is shown.

The RelA-mediated effect on turnover was confirmed by Western analysis, which, in addition, demonstrated an enhanced phosphorylation of IκBαEGFP in IL-1-stimulated cells following co-transfection (Fig. 2, *A* and *B*). The RelA-mediated effect on phosphorylation of the inhibitor protein resulted in a 2-fold increase in non-IL-1-stimulated levels and caused a 50–100% enhancement of the peak value at 5–10 min of IL-1 stimulation. In addition, these experiments showed similar but less pronounced effects on the endogenous protein.

The dependence of the RelA-induced effects on IκBα concentration, demonstrated by single cell analysis, prompted quantitation of inhibitor levels. Immunocytochemical staining of transfected cells and monitoring of red and green fluorescence demonstrated a linear relationship between total and transfected levels of the protein over a wide range of concentrations (Fig. 3, *A* and *B*). A mean transfection level of 1 fluorescent unit corresponded to an increase in cytoplasmic IκBα to about 3-fold the average endogenous levels (Fig. 3*B*). Quantitation by Western analysis of cells transfected with *pIκBαEYFP* and *pECFPrelA* showed average concentrations of 400,000 and 370,000 molecules/cell for IκBαEYFP and ECFPrelA (Fig. 3*C*), respectively, and revealed endogenous IκBα levels to be about 135,000 molecules/cell, 2.5-fold higher than that estimated for the average levels of endogenous RelA, as expected (20, 22), with all values close to the ranges demonstrated for the endogenous proteins (22).

Confocal microscopy further demonstrated retention of IκBα in the cytoplasm by RelA (Fig. 4). Thus, an increase in nuclear localization of tagged (Fig. 4*A*, *1–4*) or untagged (Fig 5*A*, *5* and *6*) inhibitor at higher expression levels (Fig. 4*A*, *3* and *5*) was not observed in the presence of a comparable amount of the NF-κB subunit (Fig. 4*A*, *4* and *6*). In addition, quantitation over a wide range of IκBαEGFP expression levels showed the effect to correlate with increasing levels of (*pCMV) relA* in a concentrationdependent manner (Fig. 4, *B* and *C*).

The RelA/IκBα interdependence was further analyzed by simultaneous observations of RelA and IκBα using cyan (ECFP) and yellow (EYFP) variants of GFP, respectively (*pECFPrelA* and *pIκBαEYFP*) (Fig. 5*A*). These experiments demonstrated that in the unstimulated state, both subunits were located in the cytoplasm. Quantitation showed that, similarly to experiments using EGFP containing constructs (20), IL-1 stimulation caused a successive increase in nuclear RelA but had no appreciable effect on cytoplasmic levels (Fig. 5*B*). Similarly, the rate of reduction of cytoplasmic inhibitor levels during activation was the same as that using the green fluorochrome, (compare Figs. 5*B* and 2*B*) and coincided with a reduction in the much lower levels of nuclear IκBα. The levels of RelA-IκBα complexes were assessed by measuring FRET using ECFPrelA as a donor and IκBαEYFP as the acceptor (34). FRET was observed in cells expressing both fusion proteins demonstrating *in vivo* association of IκBαEYFP and ECFPrelA (Fig. 5*A*, *6* and *9*), not seen in control cells, transfected with constructs containing EYFP and ECFP only (Fig. 5*A*, *3*). A reduction in FRET signal (compare *6* and *9*) following cytokine stimulation correlated with nuclear translocation of RelA (compare *4* and *7*) and a decrease in cytoplasmic IκBα (compare *5* and *8*). Both the level of FRET and of IκBα showed a steady state at about 50% after 30 min of IL-1 stimulation (Fig. 5*B*). The addition of RelA caused a concentration-dependent increase in the level of complexes over a range of inhibitor concentrations, reaching successively higher levels of saturation (Fig. 5*C*).

Analysis by immunoprecipitation of transfected cells demonstrated that RelA caused an increase in IκBα-containing complexes, both in control and IL-1-stimulated cells. Using a phosphospecific antibody, the experiments similarly demonstrated a significant increase in the level of complexed phosphorylated inhibitor in the presence of RelA (Fig. 6*A*). Transfecting the Ser^{32}/Ser^{36}-phosphodeficient mutant, however, resulted in a significant reduction in IκBα/RelA interactions, in both control and IL-1-stimulated cultures (Fig. 6*B*). Quantitation further demonstrated a correlation between effects on complex levels (1.96 ± 0.4) and phosphorylation (2.35 ± 0.58) using tagged or untagged RelA, before and after stimulation, with unaffected low levels using the phosphodeficient IκBαEGFP mutant (Fig. 6*C*).

The NF-κB/IκBα interaction was further characterized using FRET by measuring signals from transfected cells expressing a range of IκBα levels and modeling the data by noncooperative binding of ligand (IκBα) to a single class of sites (RelA). Specificity of the interaction was demonstrated by competition by increasing amounts of *pCMVrelA* or *pCMV p50*, or of a non-

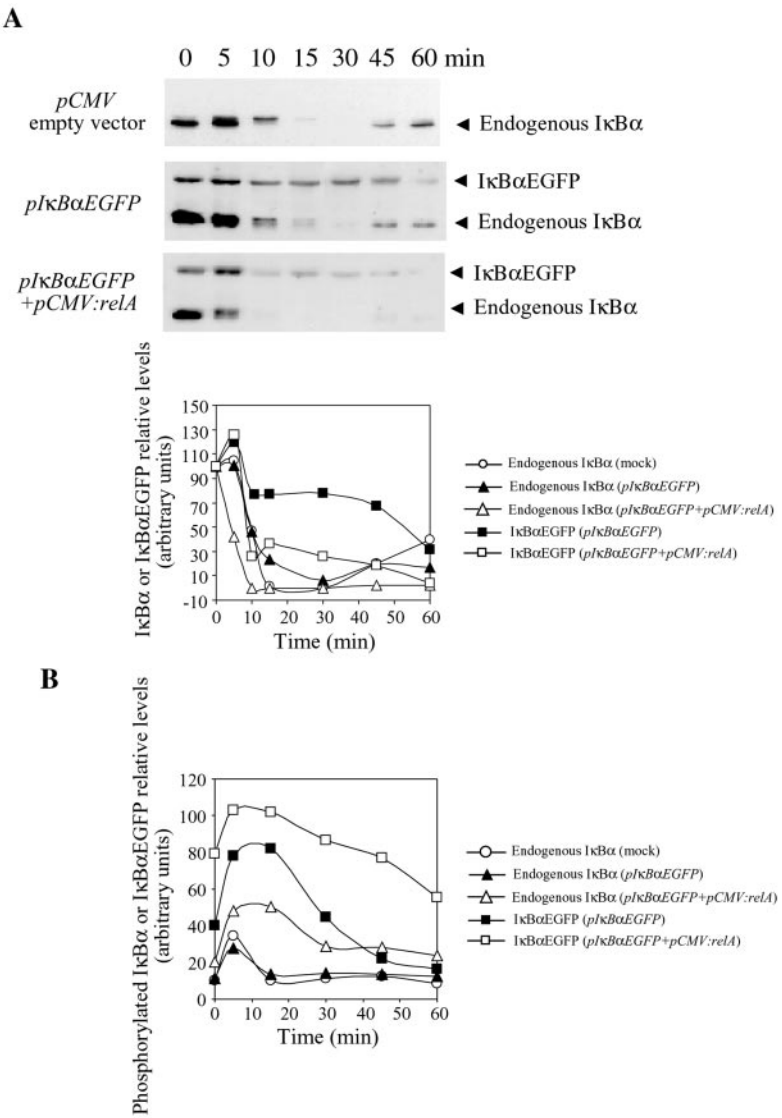

FIG. 2. **RelA enhances IL-1-induced degradation and phosphorylation of both endogenous and exogenous IκBα.** *A*, mock-transfected fibroblasts (*pCMV* empty vector) and fibroblasts transfected with IκBαEGFP alone (*pIκBαEGFP*) or together with RelA (*pIκBαEGFP* + *pCMV:relA*) were stimulated with IL-1 (10^{-9} M) for the indicated times. Cell extracts were separated on a 12.5% SDS gel, and levels of endogenous IκBα were determined by Western blotting using primary anti-rabbit polyclonal IκBα IgG. Quantitation of the level of the inhibitor was done by scanning of autoradiographs. One representative experiment of three is shown. Data are expressed relative to the initial values for each condition. *B*, cells transfected with *pIκBαEGFP* alone or co-transfected with equal amounts of *pIκBαEGFP* and *pCMV:relA* as above were stimulated with IL-1β for the times indicated. The level of phosphorylation on serine 32 of endogenous and exogenous IκBα was determined by Western blotting, using primary anti-rabbit polyclonal phospho-IκBα, and quantitated, as above. Data from one of two experiments are shown and expressed relative to initial levels of the endogenous protein.

fluorescing mutant of ECFPrelA (ECFPrelAmut) (Fig. 7*A*). This showed a dose-dependent inhibition of the FRET signal, which corresponded to about 70% at 4-fold overexpression of either of the RelA constructs, whereas co-transfection with p50 had no effect. Further, in agreement with biochemical data, shown in Fig. 6*C*, using the phosphorylation site-deficient IκBα-mutant resulted in about a 50% reduction in specific RelA binding (Fig. 7*A*).

In addition, these experiments showed that IκBα/RelA interaction (FRET) is dynamic and dependent on IκBα concentration (EYFP fluorescence), demonstrating saturation before and after incubation with IL-1 (Fig. 7*B*). A pronounced fall in the FRET signal after 30 min of IL-1 stimulation corresponded to a reduction in complex concentration to 38 ± 8%, correlating with the decrease determined by immunoprecipitation (see Fig. 6). In comparison, using the phosphonegative mutant resulted in a much decreased level of complexes, which were unaffected by IL-1 stimulation (Fig. 7*B*). Characterization of the interaction by Scatchard analysis demonstrated a pronounced (4.2 ± 1.0-fold) increase in affinity (K_a) of RelA binding to the wild type inhibitor following stimulation with the cytokine, relative to that calculated for control cultures (Fig. 7*C*). Quantitation of fusion protein levels, as in Fig. 3*C*, gave estimated affinity constants (K_a) for these interactions in the range of 10^7 to 5×10^7 M^{-1} in unstimulated cells and between 5×10^7 and 5×10^8 M^{-1} following IL-1 stimulation, respectively. In comparison, the affinity of RelA for the phosphonegative mutant was only 25% of that for the wild type and, in addition, was unaffected by cytokine activation (Fig. 7*C*).

DISCUSSION

The data presented in this report are in broad agreement with the widely accepted model based on NF-κB/IκB interdependence and regulation through IκBα phosphorylation. The real time GFP measurements on single cells, in addition, show that the IκBα/NF-κB interaction is specific, saturable, and dynamic; that the RelA-induced increase in binding relies on trafficking; and that regulation of complex formation and of the affinity of the interaction are IκBα phosphorylation-dependent.

Our data underscore the reciprocal nature of NF-κB/IκB regulation, coupled with a system in which free components successively accumulate in the nucleus with increasing levels, and bound complexes largely remain in the cytoplasm, in the resting state (20). This is reflected in the inverse correlation between the inhibitor cytoplasmic concentration and the ratio of cytoplasmic to nuclear levels and by the cytoplasmic accumulation of IκBα in the presence of excess RelA. Regulation is probably influenced by the level of the endogenous proteins and of *de novo* synthesis through autoregulation (35), since the low transfection levels of the GFP fusions, corresponding to 2–3-

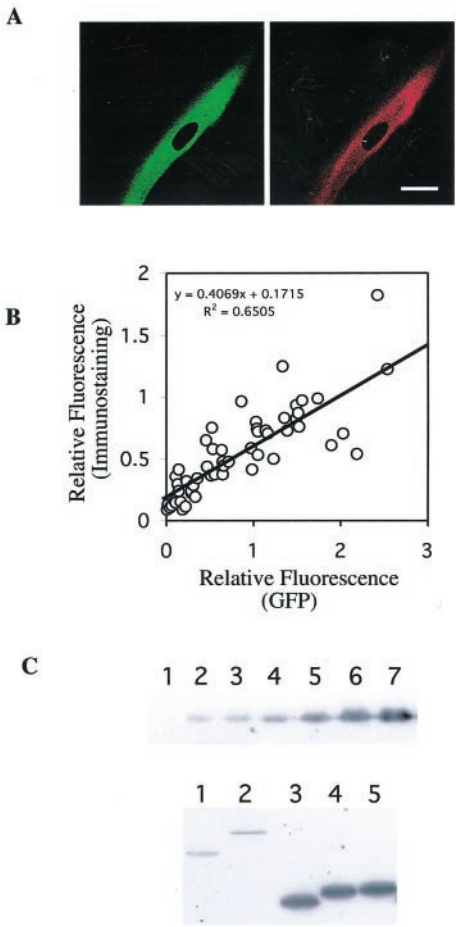

FIG. 3. **Quantitation of correlation between levels of exogenous and total IκBα.** *A*, cells transfected with *pIκBαEGFP* (*left panel*) were subjected to immunostaining using an anti-IκBα antibody and streptavidin/Texas Red (*right panel*), as described under "Experimental Procedures." *Bar*, 20 μm. *B*, the relative levels of IκBαEGFP fusion protein (GFP) and total IκBα (immunostaining) were determined and subsequently correlated by plotting green and red fluorescence for 55 individual cells expressing a range of transfection levels. *C*, Western blot of transfected proteins. *Upper panel*, *lanes 1–7*, 0, 0.3, 0.5, 1, 3, 5, and 7 ng of purified EGFP, respectively. *Lower panel*, extracts of cells transfected with IκBαEYFP (*lane 1*), ECFPrelA (*lane 2*), EGFP (*lane 3*), EYFP (*lane 4*), and ECFP (*lane 5*).

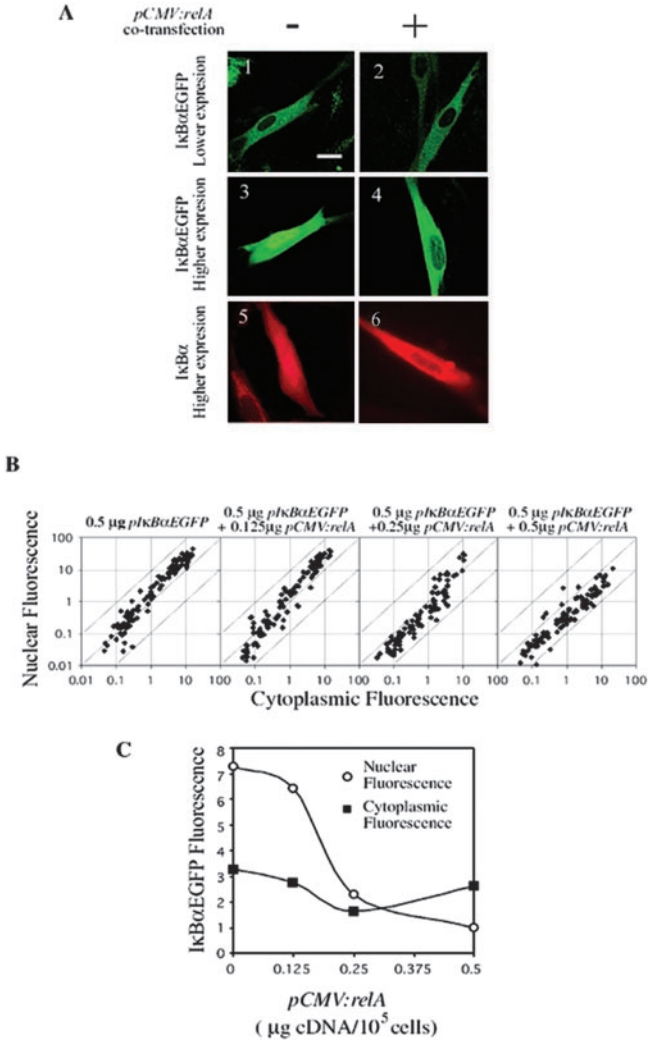

FIG. 4. **RelA regulates localization of IκBα.** *A*, confocal micrographs of fibroblasts transfected with lower (*1* and *2*) and higher (*3* and *4*) levels of *pIκBαEGFP* or higher levels of *pCMV:IκBα* (*5* and *6*), alone (*1*, *3*, and *5*) or co-transfected with *pCMV:relA* (*2*, *4*, and *6*), demonstrating increased nuclear levels of the fusion protein in cells with high levels of transfection (*3* and *5*), which are reduced in the presence of RelA (*4* and *6*). *Bar*, 20 μm. *B*, quantitation of nuclear and cytoplasmic levels of cells transfected with *pIκBαEGFP* alone or co-transfected with increasing amounts of *pCMV:relA* (as indicated), over a range of concentrations. *C*, quantitation of average nuclear and cytoplasmic fluorescence after transfection with *pIκBαEGFP* alone and together with increasing concentrations of *pCMV:relA*.

fold that of the endogenous protein, are well within the physiological range of variation (22). Thus, the successive increase in nuclear levels at higher concentrations of IκB-EGFP probably reflects titering out of endogenous NF-κB. Further, competition for the endogenous pool of NF-κB could account for the enhanced level of breakdown of IκBαEGFP and the limited effect of co-transfection at low levels of exogenous inhibitor (22).

Enhanced cytoplasmic retention of IκBα, such as that induced by RelA, has significant effects on pathway regulation (36–41).[2] This is supported by mathematical modeling, which shows that the κB system is dissipative and far from equilibrium and is at a steady state determined by dissociation of complexes, intercompartmental trafficking, and synthesis and breakdown of components (21).[3] Further, simple kinetics (Briggs-Haldane) show that saturable NF-κB/IκBα binding, under steady state conditions, can occur with apparent affinity constants much lower than those observed with pure components *in vitro*, in agreement with the lower affinities measured in our study, compared with those observed using Biocore (42).

The involvement of basal cycling in regulation (21), indicated by the slightly delayed decrease in FRET (47%) compared with that of the inhibitor fluorescence (56%) (significant at 5%), suggests a reassociation of released ECFPrelA with free IκBαEYFP prior to nuclear entry. The biological significance of transport is not likely to enhance the level of activation, since the kinetics of inhibitor reduction in the two compartments is identical (60–70%). Rather, it may constitute the basis for recruiting specific subsets of NF-κB intermediates for distinct facets of pathway regulation, such as complexes activated subsequent to nuclear translocation (36). The significance of selectivity during pathway activation is supported by the burgeoning evidence of diversity and complexity of NF-κB induction (2, 36, 41, 43–47). This further supports the notion of a system where perturbations in concentrations of signaling components and in the system steady state, such as that induced by in-

[2] L. Yang and E. E. Qwarnstrom, unpublished observations.
[3] S. K. Dower, L. Yang, and E. E. Qwarnstrom, unpublished observations.

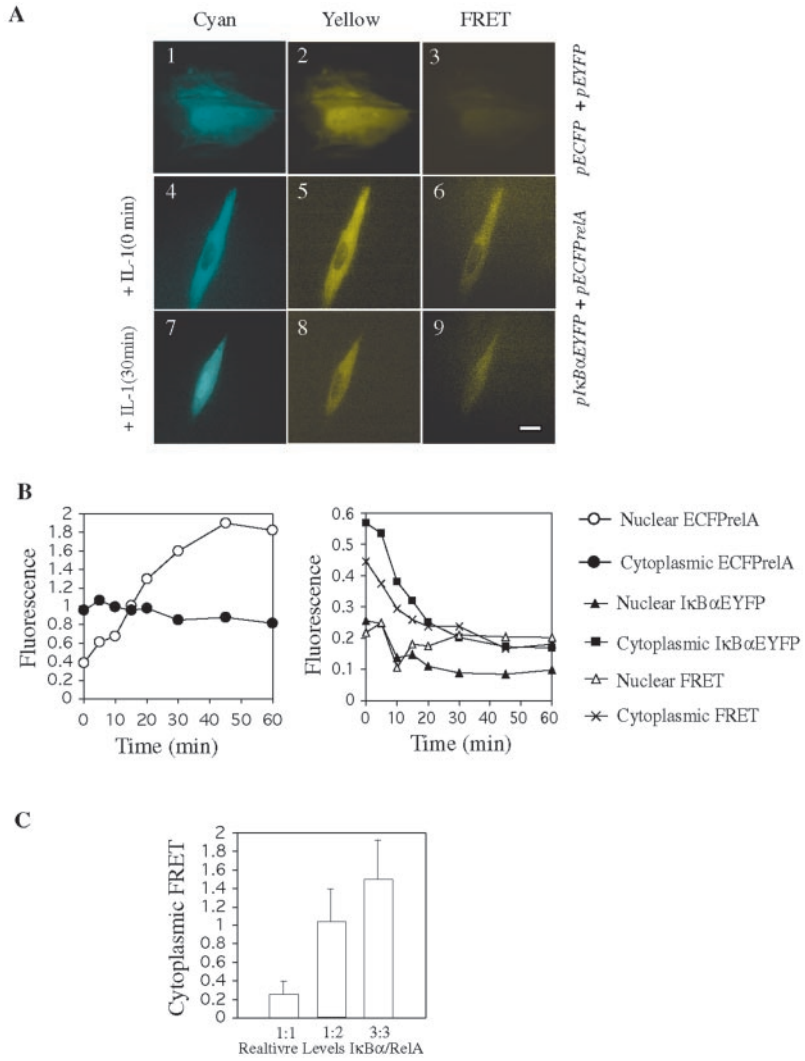

FIG. 5. **ECFPrelA regulates IκBα-EYFP complex formation in living cells.** *A*, fibroblasts were co-transfected with control constructs, *pECFP-C1* plus *pEYFP-C1* (*1–3*), or *pECFPrelA* plus *pIκBαEYFP* (*4–9*). Simultaneous analysis of RelA localization (*4* and *7*), IκBα degradation (*5* and *8*), and complex formation (*6* and *9*) during stimulation was carried out by recording cyan, yellow, and FRET images, respectively. In the unstimulated cell (*4–6*), both fusion proteins are located in the cytoplasm. 30-min stimulation with 1 nM IL-1 (*7–9*) causes an increase in nuclear levels of ECFPrelA (compare *4* and *7*), together with a reduction in cytoplasmic IκBαEYFP (compare *5* and *8*) and in the FRET signal (compare *6* and *9*). *Bar*, 20 μm. *B*, quantitation of IκBα and FRET signals in cells undergoing nuclear translocation of NF-κB, during stimulation with 1 nM IL-1β, was carried out by determining fluorescent intensity, for the respective spectra, as described under "Experimental Procedures." *Left panel*, time course of nuclear and cytoplasmic ECFPrelA fluorescence. *Right panel*, time course of FRET and IκBα fluorescence in the nucleus and cytoplasm. *C*, cytoplasmic FRET at increasing levels of RelA and IκBα over a range of concentrations, corresponding to fluorescent units in the ranges as indicated. Shown are averages ± S.E. of saturated levels of binding, calculated using mlab for three series of cells.

creased levels of RelA, can have marked effects on both the extent and mechanism of NF-κB-induced gene transcription.

Enhanced inhibitor phosphorylation in the presence of exogenous RelA is probably to some extent due to an increase in NF-κB-IκBα complexes and reflects preferential phosphorylation of complexed inhibitor by IκB kinases (48). Conversely, the pronounced reduction in RelA/IκBα binding at steady state, observed with the 32/36 mutant, demonstrated dependence of complex formation and affinity on IκBα phosphorylation, as found for interactions through the PEST domain of the protein (49). In the absence of a direct involvement of the IκBα signal-receiving domain in NF-κB interaction (42), the effects on specific binding, observed using the mutants, could be explained by changes in inhibitor conformation *in vivo*. A decrease in binding of IκBα proteins lacking the phosphorylation sites necessary for proteosome degradation (6, 31, 32), is consistent with a critical role for RelA in controlling IκBα turnover. Of the three components of the classical κB complex, RelA is present at the lowest concentration (22). Linking IκBα turnover to RelA levels will therefore optimize signals through the IκB kinases. In addition, ongoing studies suggest that further amplification through positive feedback is induced by increased activation of upstream kinases in the presence of excess RelA.[4] This is in agreement with a system based on reutilizing a limited amount of RelA through repeated cycles of IκBα binding, phosphorylation, and degradation and with continuous enhanced effects with increasing RelA concentrations.

Alterations in the level and affinity of IκBα-NF-κB complexes correlated with the rate of inhibitor degradation. With only 20% of NF-κB free of IκBα (20), a 4-fold change in complex affinity is likely to have a significant role in regulation of inhibitor turnover, subsequent to effects on basal shuttling and reduction in free NF-κB. The identical results obtained in the blocking experiments, using tagged and untagged RelA, show that the lower affinities we observe *in vivo* compared with that measured with purified proteins (41) are not artifacts of GFP tagging (50). The increase in NF-κB/IκBα affinity correlates with the enhanced cytoplasmic FRET/IκBαEYFP ratio following IL-1 stimulation, suggesting a selective process. This is also supported by the lack of a simple inverse correlation between the affinity and the level of complexes and indicates that low affinity complexes are specifically targeted for degradation during cytokine activation. The biological significance of this selection could be to facilitate a rapid release in response to a transient signal through the low affinity complexes, characterized by a high dissociation rate. The heterogeneity of NF-κB-IκBα complex affinity may thus constitute a buffer to incoming signals.

In summary, the data show that translocation, phosphorylation, and complex formation are all critical for regulation of IκBα steady state levels by NF-κB. They demonstrate that

[4] I. Evans, K. P. Ray, and E. E. Qwarnstrom, unpublished observations.

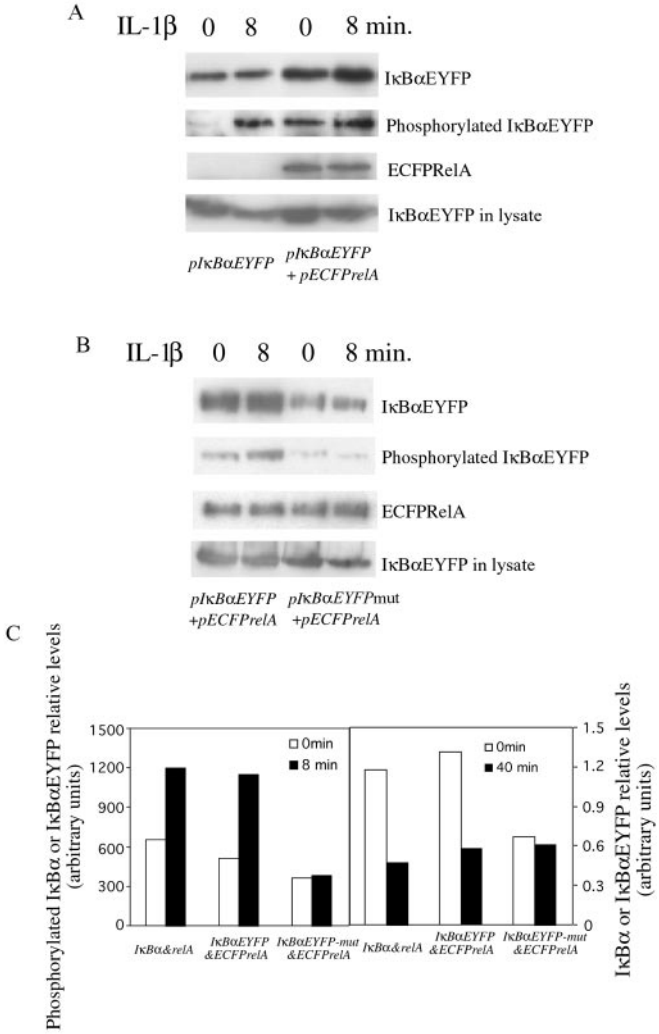

FIG. 6. **RelA induces phosphorylation-dependent complex formation.** *A*, cells transfected with IκBαEYFP alone or co-transfected with an ECFPrelA-containing construct were stimulated with IL-1 for 0 or 8 min. Extracts were subjected to immunoprecipitation using an anti-RelA antibody and separated on a 12.5% SDS gel, and the levels of RelA, IκBα, and phospho-IκBα for the various conditions were determined by Western analysis, as described under "Experimental Procedures." Similarly, the level of IκBαEYFP in the total lysate was assessed by Western analysis. One of two experiments is shown. *B*, cells were transfected with wild type IκBαEYFP or with a mutant lacking phosphorylation sites Ser^{32} and Ser^{36}, together with ECFPrelA, and stimulated with IL-1 for 0 or 8 min, as above. Complexes were immunoprecipitated following extraction by using an anti-RelA antibody, separated on a 12.5% gel, and subjected to Western analysis, as in *A*. One of three experiments is shown. *C*, levels of total and phosphorylated complexes were determined for cells transfected with untagged or fluorescence-tagged IκBα or with a fluorescence-tagged mutant IκBα lacking phosphorylation sites serine 32 and 36, together with untagged or tagged RelA as indicated, and stimulated with IL-1 for 0, 8, or 40 min. Quantitation was carried out following immunoprecipitation, gel electrophoresis, and Western analysis, as above, by scanning autoradiograms. *Left panel*, the level of phosphorylated complexes at 0 and 8 min. Data represent the average of three experiments and are expressed relative to total IκBα in the lysate. *Right panel*, the total level of complexes at 0 and 40 min. One representative experiment of three is shown, with data expressed relative to total RelA.

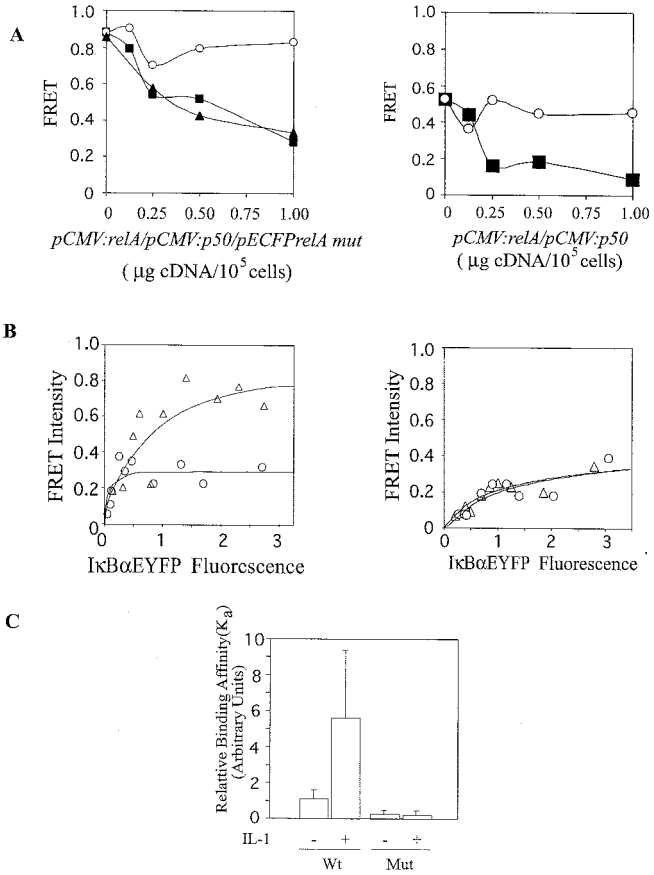

FIG. 7. **IκBα phosphorylation regulates the level and affinity of IκBα-RelA complexes.** *A*, inhibition of IκBα/RelA interaction was assessed by transfecting cells with *pIκBαEYFP* (*left panel*, wild type IκBα) or *pIκBαEYF-mut* (*right panel*, phosphodeficient mutant) (0.25 μg/2.5 × 10^4 cells) and *pECFPrelA* (0.25 μg/2.5 × 10^4 cells) together with increasing amounts (0–1 μg/2.5 × 10^4 cells) of *pCMV:relA* (■), *pCMV:p50* (○), or a mutant, *pECFPrelA*, lacking the cyan fluorescent site (▲). One of two experiments for each condition is shown. *B*, an analysis of binding of IκBαEYFP with ECFPrelA before and after 30-min stimulation with IL-1β. Each data point represents the average of readings from three cells. *Left panel*, binding before and after IL-1 stimulation in cells co-transfected with the wild type IκBαEYFP construct and ECFPrelA. *Right panel*, binding before and after IL-1 stimulation, in cells co-transfected with the phosphorylation site-deficient IκBαEYFP mutant and ECFPrelA. One representative experiment of four and two, respectively is shown for the conditions. △, control cultures; ○, following 30 min of IL-1 stimulation. *C*, relative level of affinity of RelA interactions with the wild type (*Wt*) and the phosphodeficient mutant (*Mut*) of IκBα, respectively, in control and in cells stimulated with IL-1 for 30 min, as indicated. Scatchard analysis of experiments as in *B* were carried out using mlab, and data are expressed relative to the affinity constant (K_a) in unstimulated cells transfected with equal amounts of ECFPrelA and wild type IκBαEYFP. Shown are the averages of four (wild type) and two (mutant) experiments, respectively.

IκBα/NF-κB binding is dynamic, saturable at steady state, and phosphorylation-dependent. They also show that both the extent and the affinity of the IκBα/NF-κB interaction play a role in system regulation, affecting both basal levels and those induced in response to incoming signals. The multifaceted effects of RelA on the concentration-dependent limitation of inhibitor turnover thus constitute a complex feedback loop, with effects on the system steady state and with expected significance for the specificity and level of NF-κB activity.

Acknowledgments—The IκB (*pGEX.IκBctag*) was a generous gift from Prof. Ronald Hay. *pRSV-NF-κB1* (p50) and *Bluescript-RelA* (p65) were obtained through the AIDS Research and Reference Reagent Program, Division of AIDS, NIAID National Institutes of Health, from Dr. Gary Nabel and Dr. Neil Perkins. We also thank Dr. Steve Poole for the kind gift of IL-1β and Prof. Steve Dower for useful discussions. The confocal microscopy analyses were carried out using the facility in the Section of Functional Genomics, University of Sheffield, UK.

REFERENCES

1. Kopp, E. B., and Ghosh, S. (1995) *Adv. Immunol.* **58,** 1–27
2. Baeuerle, P. A., and Baltimore, D. (1996) *Cell* **87,** 13–20
3. Christman, J. W., Lancaster, L. H., and Blackwell, T. S. (1998) *Intensive Care Med.* **24,** 1131–1138

4. Ghosh, S., May, M. J., and Kopp. E. B., (1998) *Annu. Rev. Immunol.* **16,** 225–260
5. Israel, A. (1995) *Trends Genet.* **11,** 203–205
6. Beg, A. A., and Baldwin, A. S., Jr. (1993) *Genes Dev.* **7,** 2064–2070
7. Beg, A. A., Ruben, S. M., Scheinman, R. I., Haskill, S., Rosen, C. A., and Baldwin, A. S., Jr. (1992) *Genes Dev.* **6,** 1899–1913; Correction (1992) *Genes Dev.* 2664–2665
8. Beg, A. A., and Baltimore, D. (1996) *Science* **274,** 782–784
9. Qwarnstrom, E. E., Ostberg, C. O., Turk, G. L., Richardson, C. A., and Bomsztyk, K. (1994) *J. Biol. Chem.* **269,** 30765–30768
10. DiDonato, J., Mercurio, F., Rosette, C., Wu-Li, J., Suyang, H., Ghosh, S., and Karin, M. (1996) *Mol. Cell. Biol.* **16,** 1295–1304
11. Mercurio, F., Zhu, H., Murray, B. W., Shevchenko, A., Bennett, B. L., Li, J., Young, D. B., Barbosa, M., Mann, M., Manning, A., and Rao, A. (1997) *Science* **278,** 860–866
12. Woronicz, J. D., Gao, X., Cao, Z., Rothe, M., and Goeddel, D. V. (1997) *Science* **278,** 866–869
13. Zandi, E., Rothwarf, D. M., Delhase, M., Hayakawa, M., and Karin, M. (1997) *Cell* **91,** 243–252
14. Karin, M. (1999) *J. Biol. Chem.* **274,** 27339–27342
15. Van Antwerp, D. J., and Verma, I. M. (1996) *Mol. Cell. Biol.* **16,** 6037–6045
16. Verma, I. M., Stevenson, J. K., Schwarz, E. M., Vanantwerp, D., and Miyamoto, S. (1995) *Genes Dev.* **9,** 2723–2735
17. Rodriguez, M. S., Michalopoulos, I., Arenzana-Seisdedos, F., and Hay, R. T. (1995) *Mol. Cell. Biol.* **15,** 2413–2419
18. Yang, L., Chen, H., and Qwarnstrom. E. (2001) *Biochem. Biophys. Res. Commun.* **285,** 603–608
19. Duckett, C. S., Perkins, N. D., Kowalik, T. F., Schmid, R. M., Huang, E. S., Baldwin, A. S., Jr., and Nabel. G. J. (1993) *Mol. Cell. Biol.* **13,** 1315–1322
20. Carlotti, F., Chapman, R., Dower, S. K., and Qwarnstrom, E. E. (1999) *J. Biol. Chem.* **274,** 37941–37949
21. Carllotti, F., Dower, S. K., and Qwarnstrom, E. E. (2000) *J. Biol. Chem.* **275,** 41028–41034
22. Schooley, K., Zhu, P., Dower, S. K., and Qwarnstrom, E. E. (2003) *Biochem. J.* **369,** 331–339
23. Laemmli, U. K. (1970) *Nature* **227,** 680–685
24. Clegg, R. M. (1995) *Curr. Opin. Biotechnol.* **6,** 103–110
25. Herman, B. (1989) *Methods Cell Biol.* **30,** 219–243
26. Szollosi, J., Damjanovich, S., and Matyus, L. (1998) *Cytometry* **34,** 159–179
27. Adams, S. R., Harootunian, A. T., Buechler, Y. J., Taylor, S. S., and Tsien, R. Y. (1991) *Nature* **349,** 694–697
28. Damelin, M., and Silver, P. A. (2000) *Mol. Cell* **5,** 133–140
29. Mochizuki, N., Yamashita, S., Kurokawa, K., Ohba, Y., Nagai, T., Miyawaki, A., and Matsuda, M. (2001) *Nature* **411,** 1065–1067
30. Zaccolo, M., and Pozzan, T. (2000) *IUBMB Life* **49,** 375–379
31. Brown, K., Gerstberger, S., Carlson, L., Franzoso, G., and Siebenlist, U. (1995) *Science* **267,** 1485–1491
32. Chen, Z., Hagler, J., Palombella, V. J., Melandri, F., Scherer, D., Ballard, D., and Maniatis, T. (1995) *Genes Dev.* **9,** 1586–1597
33. Li, X., Fang, Y., Zhao, X., Jiang, X., Duong, T., and Kain., S. R. (1999) *J. Biol. Chem.* **274,** 21244–21250
34. Mahajan, N. P., Linder, K., Berry, G., Gordon, G. W., Heim, R., and Herman, B. (1998) *Nat. Biotechnol.* **16,** 547–552
35. Chiao, P. J., Miyamoto, S., and Verma, I. M. (1994) *Proc. Natl. Acad. Sci. U. S. A.* **91,** 28–32
36. Johnson, C., Van Antwerp, D., and Hope, T. J. (1999) *EMBO J.* **18,** 6682–6693
37. Huang, T. T., Kudo, N, Yoshida, M., and Miyamotot, S. (2000) *Proc. Natl. Acad. Sci. U. S. A.* **97,** 1014–1019
38. Tam, W. F., Lee, L. H., Davis, L., and Sen, R. (2000) *Mol. Cell. Biol.* **20,** 2269–2284
39. Turpin, P., Hay, R. T., and Dargemont, C. (1999) *J. Biol. Chem.* **274,** 6804–6812
40. Prigent, M., Barlat, I., Langen, H., and Dargemont, C. (2000) *J. Biol. Chem.* **275,** 36441–36449
41. Caunt, C. J., Kiss-Toth, E., Carlotti, F., Chapman, R., and Qwarnstrom, E. E. (2001) *J. Biol. Chem.* **276,** 6280–6288
42. Malek, S., Huxford, T., and Ghosh, G. (1998) *J. Biol. Chem.* **273,** 25427–25435
43. Arenzana-Seisdedos, F., Thompson, J., Rodriguez, M. S., Bachelerie, F., Thomas, D., and Hay, R. T. (1995) *Mol. Cell. Biol.* **15,** 2689–2696
44. Jefferies, C., Bowie, A., Brady, G., Cooke, E. L., Li, X., and O'Neill, L. A. (2001) *Mol. Cell. Biol.* **21,** 4544–4552
45. Rodriguez, M. S., Thompson, J., Hay, R. T., and Dargemont, C. (1999) *J. Biol. Chem.* **274,** 9108–9115
46. Zhong, H., Voll, R. E., and Ghosh, S. (1998) *Mol. Cell* **1,** 661–671
47. Hoffman, A., Levchenko, A., Scott, M., and Baltimore, D. (2002) *Science* **298,** 1241–1245
48. Zandi, E., Chen, Y., and Karin, M. (1998) *Science* **281,** 1360–1363
49. Phelps, C. B., Sengchanthalangsy, L. Huxford, T., and Ghosh, G. (2000) *J. Biol. Chem.* **275,** 29846–29846
50. Schmidt, J. A., Birbach, A., Hofer-Warbinek, R., Pengg, M., Burner, U., Furtmuller, P. G., Binder, B. R., and de Martin, R. (2000) *J. Biol. Chem.* **275,** 17035–17042